Facile activation of hydrogen by unsaturated platinum–osmium carbonyl cluster complexes

Richard D. Adams *, Burjor Captain, Lei Zhu

*Department of Chemistry and Biochemistry, University of South Carolina, Columbia, SC 29208, United States*

Abstract

The electronically unsaturated cluster complex $Os_3Pt_2(CO)_{10}(PBu_3^t)_2$ (**10**) was obtained from the reaction of $Os_3(CO)_{10}(NCMe)_2$ with $Pt(PBu_3^t)_2$. Three side products: $PtOs_3(CO)_{10}(PBu_2^t)CMe_2CH_2(\mu\text{-}H)$ (**13**), $Os_3(CO)_{10}(PBu_3^t)_2$ (**14**) and $Pt_2Os_3(CO)_{10}(PBu_3^t)(PBu_2^t)$ $CMe_2CH_2(\mu\text{-}H)$ (**15**) were also obtained from this reaction. The three osmium atoms in **10** lie in the equatorial plane of a trigonal bipyramid. The platinum atoms occupy the apical positions. When heated, compound **10** was converted to **15** by metallation of one of the methyl groups of one of the PBu_3^t ligands at the platinum atom to which it is coordinated. The platinum atom then shifted to an edge of the Os_3 triangle by cleaving one of its Pt–Os bonds. Compound **13** also contains a metallated PBu_3^t ligand attached to the platinum atom of the tetrahedral $PtOs_3$ cluster. Compound **10** reacts with hydrogen at 0 °C to yield the di- and tetra-hydrido compounds $Os_3Pt_2(CO)_{10}(PBu_3^t)_2(\mu\text{-}H)_2$ (**11**) and $Os_3Pt_2(CO)_{10}(PBu_3^t)_2(\mu\text{-}H)_4$ (**12**) with the hydrido ligands bridging Os–Pt and Os–Os bonds. With each addition of hydrogen, one of the platinum atoms in the cluster was shifted to an edge of the Os_3 triangle. When solutions of **12** at 25 °C were purged with nitrogen, hydrogen was eliminated and the compounds **10** and **11** were regenerated. The electronic structures of **10** and **11** were also investigated by Fenske–Hall molecular orbital theory. When compound **10** was exposed to hydrogen for 2.5 h, compound **12** was formed together with the new tetranuclear metal cluster complexes $PtOs_3(CO)_{10}(PBu_3^t)(\mu\text{-}H)_2$ (**16**), $PtOs_3(CO)_9(PBu_3^t)(\mu\text{-}H)_4$ (**17**) and $PtOs_3(CO)_8(PBu_3^t)_2(\mu\text{-}H)_4$ (**18**). Compounds **16–18** contain tetrahedrally shaped clusters of four metal atoms with bridging hydrido ligands. All new compounds were characterized structurally by single-crystal X-ray diffraction methods.

1. Introduction

In recent studies, we have shown that the compounds $M(PBu_3^t)_2$, M = Pd or Pt are excellent reagents for the addition of $M(PBu_3^t)$ groups to the metal–metal bonds of transition metal carbonyl cluster complexes [1–3]. In most cases the $M(PBu_3^t)$ group is added to just two metal atoms to form an edge-bridging group. For example, the reaction of $Ru_3(CO)_{12}$ with an excess of $Pd(PBu_3^t)_2$ yielded the tris-$Pd(PBu_3^t)$ adduct, $Ru_3(CO)_{12}[Pd(PBu_3^t)]_3$ (**1**) that contains a $Pd(PBu_3^t)$ group on each of the three Ru–Ru bonds of the original molecule of $Ru_3(CO)_{12}$, Eq. (1) [1].

(1)
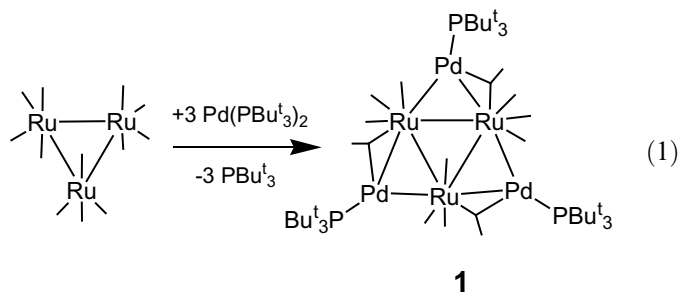
The reaction of $Os_3(CO)_{12}$ with $Pt(PBu_3^t)_2$ yielded a series of three adducts, $Os_3(CO)_{12}[Pt(PBu_3^t)]_x$, **2–4**, x = 1–3, containing one–three edge bridging $Pt(PBu_3^t)$ groups on the Os–Os bonds, Eq. (2) [2].

---

* Corresponding author.
  E-mail address: Adams@mail.chem.sc.edu (R.D. Adams).

(2)
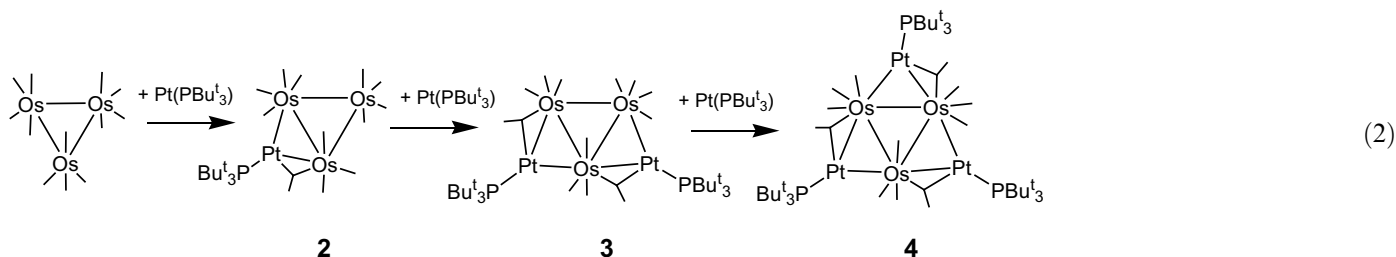
In some cases, the Pt(PBu^t) group can be inserted into the metal–metal bond. For example, the reaction of Re$_3$(CO)$_{12}$(μ-H)$_3$ with Pt(PBu$_3^t$)$_2$ yielded the mono adduct PtRe$_3$(CO)$_{12}$(PBu$_3^t$)(μ-H)$_3$ (5) formed by the insertion of a Pt(PBu$_3^t$) group into one of the hydride-bridged Re–Re bonds, Eq. (3) [4]. This reaction is partially reversible.

(3)
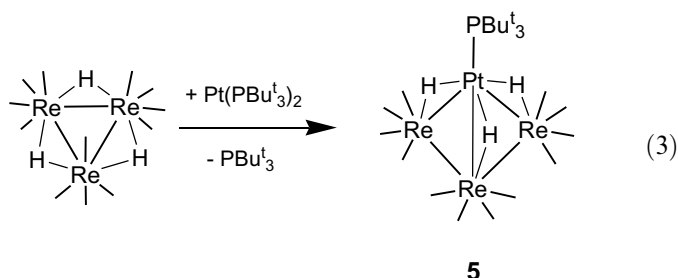
In the reaction of Re$_2$(CO)$_{10}$ with Pt(PBu$_3^t$)$_2$, three Pt(PBu$_3^t$) groups were inserted into the Re–Re bond to yield pentanuclear trigonal bipyramidal platinum–rhenium complex Pt$_3$Re$_2$(CO)$_6$(PBu$_3^t$)$_3$ (6) that is unsaturated by the unusual amount of 10 electrons [5].

Interest in the use of hydrogen for energy-related purposes [6] has renewed interests in the interactions of hydrogen with metal-containing materials for storage and for the development of new catalysts for hydrogen transformations [7,8]. The activation of hydrogen by metal complexes has received considerable attention [9]. Recent studies have shown the electronically unsaturated polynuclear metal complexes are able to activate hydrogen, some times reversibly under mild conditions [5,10]. Interestingly, it was found that compound 6 readily adds 3 equiv. of hydrogen sequentially at room temperature to yield the series of hydrido platinum–rhenium complexes Pt$_3$Re$_2$(CO)$_6$(PBu$_3^t$)$_3$(μ-H)$_x$, 7–9, x = 2, 4, 6, that have bridging hydrido ligands on the Re–Pt bonds, Eq. (4) [5]. The addition of hydrogen to 6 adds electrons to the complex and reduces the electronic unsaturation in the cluster.

We have now found that the reaction of the lightly-stabilized triosmium complex Os$_3$(CO)$_{10}$(NCMe)$_2$ with Pt(PBu$_3^t$)$_2$ yields the new pentanuclear platinum–osmium complex Pt$_2$Os$_3$(CO)$_{10}$(PBu$_3^t$)$_2$, 10 by the addition of two Pt(PBu$_3^t$) groups to the Os$_3$(CO)$_{10}$(NCMe)$_2$ and the loss of the two NCMe ligands. The two Pt(PBu$_3^t$) groups in 10 have adopted triply-bridging positions on opposite sides of the Os$_3$ triangle. Compound 10 is also electronically unsaturated by the amount of four electrons. Nevertheless, it still reacts with hydrogen under unusually mild conditions, namely 0 °C, to form a series of two new products Pt$_2$Os$_3$(CO)$_{10}$(PBu$_3^t$)$_2$(μ-H)$_2$ (11), and Pt$_2$Os$_3$(CO)$_{10}$(PBu$_3^t$)$_2$(μ-H)$_4$ (12), containing two and four hydrido ligands, respectively. Interestingly, these hydrogen addition reactions can be reversed partially by purging their solutions with nitrogen at 25 °C. Herein, we report our studies of the synthesis and structural characterization of Pt$_2$Os$_3$(CO)$_{10}$(PBu$_3^t$)$_2$ (10), its reactions with hydrogen, and the nature of the products that have been obtained from these reactions. A preliminary report of this work was published recently [11].

2. Experimental

2.1. General data

All the reactions were performed under a nitrogen atmosphere by using Schlenk techniques. Reagent grade solvent CH$_2$Cl$_2$ was dried by the standard procedures and was freshly distilled before use. Infrared spectra were recorded on an AVATAR 360 FT-IR spectrophotometer. ^{1}H NMR and ^{31}P NMR were recorded on a Varian Mercury 400 spectrometer operating at 400 and 162 MHz, respectively. ^{31}P{^{1}H} NMR spectra were externally referenced against 85% ortho-H$_3$PO$_4$. Variable temperature ^{1}H NMR spectra were recorded on a Varian Innova 500 spectrometer

(4)
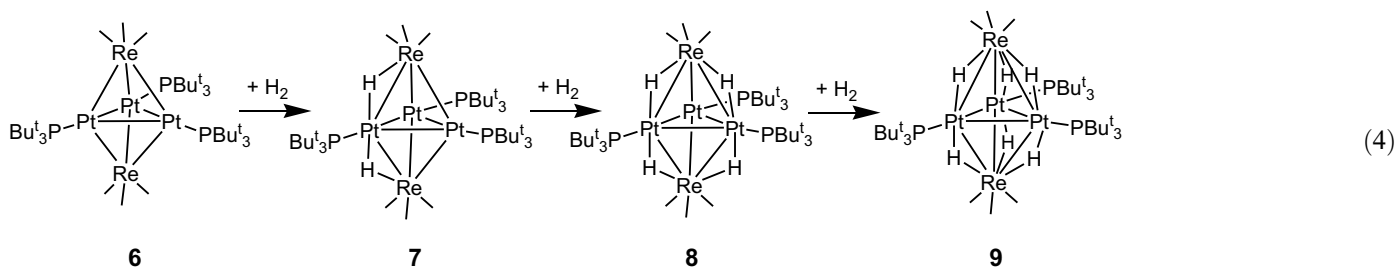
operating at 500 MHz. Mass spectrometric measurements performed by direct exposure probe using electron impact ionization (EI) were made on a VG 70S instrument. Electrospray mass spectrometric measurements were obtained on a MicroMass Q-Tof spectrometer. Elemental analyses were performed by Desert Analytics (Tucson, AZ). $Os_3(CO)_{10}(NCMe)_2$ was prepared according to the previously reported procedure [12]. $Pt(PBu_3^t)_2$ and PBu_3^t were purchased from STREM, and were used without further purification. Product separations were performed by TLC in air on Analtech 0.25 mm silica gel 60 Å F254 glass plates.

2.2. Reaction of $Os_3(CO)_{10}(NCMe)_2$ with $Pt(PBu_3^t)_2$

A 45.0 mg amount of $Os_3(CO)_{10}(NCMe)_2$ (0.048 mmol) was dissolved in 20 mL CH_2Cl_2 in a 50 mL three-neck flask. The solution was cooled to 0 °C in an ice bath and a 58.0 mg amount of $Pt(PBu_3^t)_2$ (0.096 mmol) added. The reaction mixture was stirred at 0 °C for 4 h. The solvent was then removed *in vacuo* and the product was separated by TLC by using a 5/1 hexane/methylene chloride solvent mixture to yield in order of elution: 4.2 mg (7%) of grey $PtOs_3(CO)_{10}(PBu_2^t)CMe_2CH_2(\mu-H)$ (**13**), 4.8 mg (8%) of red $Os_3(CO)_{10}(PBu_3^t)_2$ (**14**), 11 mg (14%) of grey $Pt_2Os_3(CO)_{10}(PBu_3^t)(PBu_2^t)CMe_2CH_2(\mu-H)$ (**15**) and 16 mg (20%) of green $Pt_2Os_3(CO)_{10}(PBu_3^t)_2$ (**10**). Compound **15** was reported previously as a side product from the reaction of $Os_3(CO)_{12}$ with $Pt(PBu_3^t)_2$ [13]. Spectral data for **10**: IR ν_{CO} (cm^{-1} in CH_2Cl_2): 2049 (w), 2016 (s), 1996 (s), 1950 (w, sh), 1792 (w). ^{1}H NMR (in CD_2Cl_2): $\delta = 1.09$ (d, 54H, CH_3, $^3J_{P-H} = 13$ Hz). $^{31}P\{^1H\}$ NMR (in CD_2Cl_2): $\delta = 124.3$ (s, 1P, $^1J_{Pt-P} = 5447$ Hz). Anal. Calc.: C, 24.80; H, 3.28. Found: C, 24.77; H, 3.17%. Spectral data for **13**: IR ν_{CO} (cm^{-1} in CH_2Cl_2): 2077 (m), 2049 (vs), 2024 (s), 1997 (s), 1981 (m, sh), 1844 (w). ^{1}H NMR (in CD_2Cl_2): $\delta = 1.63$ (d, 2H, CH_2, $^3J_{P-H} = 13$ Hz), 1.41 (d, 18H, $^3J_{P-H} = 14$ Hz), 1.39 (d, 6H, $^3J_{P-H} = 13$ Hz), −9.43 (d, 1H, $^1J_{Pt-H} = 13$ Hz). Mass spectrum: EI-MS showed the parent ion at $m/z = 1248$. The observed isotope pattern is consistent with the Os_3Pt metal composition. Spectral data for **14**: IR ν_{CO} (cm^{-1} in CH_2Cl_2): 2079 (w), 2072 (w), 2009 (s), 1983 (s), 1935 (m). ^{1}H NMR (in CD_2Cl_2): $\delta = 1.55$ (s, br ~28 Hz $\Delta\nu_{1/2}$). $^{31}P\{^1H\}$ NMR (in CD_2Cl_2): $\delta = 76.7$. Mass Spectrum: ES$^+$/MS m/z for M$^+$ showed the parent ion at $m/z = 1256$.

2.3. Preparation of $Os_3(CO)_{10}(PBu_3^t)_2$ (14)

A 15 mg of $Os_3(CO)_{10}(NCMe)_2$ (0.016 mmol) was dissolved in 10 mL benzene in a 50 mL three-neck flask and an excess amount of PBu_3^t was added. The reaction was heated to reflux for 10 min and the solvent was then removed in vacuo. The product was separated by TLC by using a 5/1 hexane/methylene chloride solvent mixture to yield 15 mg (75%) of red **14**.

2.4. Preparation of $Pt_2Os_3(CO)_{10}(PBu_3^t)_2(\mu-H)_2$ (11)

A 9.5 mg amount of **10** (0.0058 mmol) was dissolved in 20 mL CH_2Cl_2 in a 50 mL three-neck flask and the solution was cooled to 0 °C in an ice bath. Hydrogen was then purged through the solution for 10 min. The solvent was removed *in vacuo* and the product was isolated by TLC by using a 5/1 hexane/methylene chloride solvent mixture to yield an 8.8 mg (93%) of **11**. Spectral data for **11**: IR ν_{CO} (cm^{-1} in CH_2Cl_2): 2067 (m), 2042 (m), 2010 (m), 1992 (s), 1944(w, br). ^{1}H NMR (in $CDCl_3$): $\delta = 1.39$ (d, 27H, CH_3, $^3J_{P-H} = 13$ Hz), 1.34 (d, 27H, CH_3, $^3J_{P-H} = 13$ Hz), −10.49 (d, 1H, hydride, $^1J_{Pt-H} = 559$ Hz, $^2J_{P-H} = 11$ Hz), −10.71 (s, 1H, hydride, $^2J_{Pt-H} = 23$ Hz, $^2J_{Pt-H} = 25$ Hz). $^{31}P\{^1H\}$ NMR (in $CDCl_3$): $\delta = 117.6$ (s, 1P, $^1J_{Pt-P} = 2787$ Hz), 112.2 (s, 1P, $^1J_{Pt-P} = 5579$ Hz). Mass Spectrum: EI-MS showed the parent ion at $m/z = 1648$. The observed isotope pattern is consistent with the metal composition Os_3Pt_2.

2.5. Preparation of $Pt_2Os_3(CO)_{10}(PBu_3^t)_2(\mu-H)_4$ (12)

A 9.0 mg amount of **10** (0.0055 mmol) was dissolved in 20 mL CH_2Cl_2 in a 50 mL three-neck flask and the solution was cooled to 0 °C with an ice bath. Hydrogen was then purged through the solution for 1 h. The solvent was removed *in vacuo* and the product was isolated by TLC by using 5/1 hexane/methylene chloride solvent mixture to yield 5.7 mg (63%) of **12**. Spectral data for **12**: IR ν_{CO} (cm^{-1} in CH_2Cl_2): 2062 (m), 2027 (s), 2000 (w), 1960 (m). ^{1}H NMR (in $CDCl_3$): $\delta = 1.52$ (d, 54H, CH_3, $^3J_{P-H} = 13$ Hz), −9.01 (m, 2H, hydride, $^2J_{H-H} = 2.6$ Hz, $^1J_{Pt-H} = 421$ Hz), −16.65 (m, 2H, hydride, $^2J_{H-H} = 2.6$ Hz, $^2J_{Pt-H} = 23$ Hz). $^{31}P\{^1H\}$ NMR (in $CDCl_3$): $\delta = 92.0$ (s, 1P, $^1J_{Pt-P} = 2749$ Hz). Anal. Calc.: C, 25.62; H, 3.73. Found: C, 25.96; H, 3.40%.

2.6. Conversion of 11 to 12

A 6.4 mg amount of **11** (0.0039 mmol) was dissolved in 15 mL CH_2Cl_2 in a 50 mL three-neck flask and the solution was cooled to 0 °C in an ice bath. Hydrogen was purged through the solution for 80 min. The solvent was removed *in vacuo* and the product was isolated by TLC by using 5/1 hexane/methylene chloride solvent mixture to yield a 4.4 mg (69%) of **12**.

2.7. Elimination of hydrogen from 12

(a) An 11 mg amount of **12** (0.0067 mmol) was dissolved in 15 mL benzene solvent in a 25 mL reaction flask in a water bath at 25 °C. Nitrogen was bubbled into the solution and a vacuum was subsequently applied every 30 min to remove the hydrogen that was released. After 10 h the solvent was removed *in vacuo* and the mixture was separated by TLC by using 6/1 hexane/methylene chloride solvent mixture to yield 3.6 mg (33%) amount of

11, 2.4 mg (22%) amount of **10**. 3.1 mg (28%) amount of **12** was recovered.

(b) An 18 mg amount of **12** (0.011 mmol) was placed in a NMR tube and then dissolved in CD_2Cl_2 solvent under nitrogen atmosphere. The sample was then placed in a water bath at 35 °C. ^{1}H and ^{31}P NMR spectra were recorded after 1 h and 3 h. Resonances for compounds **10**, **11** and hydrogen, $\delta = 4.60$, formed and grew in intensity with time.

2.8. Conversion of **10** to **15**

An 11 mg amount of **10** (0.0067 mmol) was dissolved in 25 mL hexane in a 50 mL three-neck flask and the solution was then heated to reflux for 30 min. The solvent was removed *in vacuo* and the products were isolated by TLC by using 6/1 hexane/methylene chloride solvent mixture to yield a 5.5 mg (50%) of **15**.

2.9. Preparation of $PtOs_3(CO)_{10}(PBu_3^t)(\mu\text{-}H)_2$ (**16**), $PtOs_3(CO)_9(PBu_3^t)(\mu\text{-}H)_4$ (**17**) and $PtOs_3(CO)_8(PBu_3^t)_2(\mu\text{-}H)_4$ (**18**)

A 11 mg amount of **10** (0.0067 mmol) was dissolved in 20 mL CH_2Cl_2 in a 50 mL three-neck flask and the solution was cooled to 0 °C in an ice bath. Hydrogen was then purged through the solution for 2.5 h. The solvent was removed *in vacuo* and the products were separated by TLC by using 5/1 hexane/methylene chloride solvent mixture to yield in order of elution: 0.5 mg amount (6%) of **17**, 0.8 mg (8%) of **18**, 5.2 mg (47%) of **12** and a 1.5 mg amount (19%) of **16**. Spectral data for **16**: IR v_{CO} (cm^{-1} in CH_2Cl_2): 2078 (w), 2047 (s), 2016 (m), 1989 (m), 1975 (w, sh), 1954 (w, sh), 1942 (w, sh). ^{1}H NMR (in CDCl$_3$): $\delta = 1.38$ (d, 27H, CH_3, $^{3}J_{P-H} = 13$ Hz), -7.24 (s, 1H, hydride), -8.14 (d, 1H, hydride, $^{1}J_{P-H} = 573$ Hz). $^{31}P\{^{1}H\}$ NMR (in CDCl$_3$): $\delta = 116.6$ (s, 1P, $^{1}J_{Pt-P} = 2613$ Hz). Mass spectrum: EI-MS showed the parent ion at $m/z = 1250$ with ions $1250 - 28x$, $x = 1–10$ corresponding to the loss of each of 10 CO ligands. The observed isotope distribution pattern is consistent with the Os_3Pt metal composition. Spectral data for **17**: IR v_{CO} (cm^{-1} in CH_2Cl_2): 2090 (w), 2066 (s), 2041 (s), 2001 (m), 1970 (w, sh). ^{1}H NMR (in CDCl$_3$): $\delta = 1.37$ (d, 27H, CH_3, $^{3}J_{P-H} = 13$ Hz), -10.72 (d, 2H, hydride, $^{1}J_{Pt-H} = 759$ Hz), -16.62 (d, 2H, hydride, $^{2}J_{Pt-H} = 14$ Hz, $^{3}J_{P-H} = 1.5$ Hz). $^{31}P\{^{1}H\}$ NMR (in CDCl$_3$): $\delta = 122.8$ (s, 1P, $^{1}J_{Pt-P} = 3206$ Hz). Mass Spectrum: EI-MS showed the parent ion at $m/z = 1224$ with ions $1224 - 28x$, $x = 1–9$ corresponding to the loss of each of nine CO ligands. Spectral data for **18**: IR v_{CO} (cm^{-1} in CH_2Cl_2): 2063 (m), 2029 (s), 2005 (m), 1981 (m), 1959 (m), 1938 (w, sh). ^{1}H NMR (in CDCl$_3$): $\delta = 1.48$ (d, 27H, CH_3, $^{3}J_{P-H} = 13$ Hz), 1.40 (d, 27H, CH_3, $^{3}J_{P-H} = 13$ Hz), -10.18 (dd, 2H, hydride, $^{2}J_{P-H} = 9.7$ Hz, $^{3}J_{P-H} = 1.5$ Hz, $^{1}J_{Pt-H} = 755$ Hz), -13.96 (d, 2H, hydride, $^{2}J_{P-H} = 6.4$ Hz, $^{2}J_{Pt-H} = 13$ Hz). $^{31}P\{^{1}H\}$ NMR (in CDCl$_3$): $\delta = 81.5$ (d, 1P, $^{3}J_{P-P} = 30$ Hz), 124.2 (d, 1P, $^{1}J_{Pt-P} =$ 3370 Hz, $^{3}J_{P-P} = 30$ Hz). Mass Spectrum: EI-MS showed the ion at m/z 1396, M$^{+}-2$H.

2.10. Conversion of **16** to **17**

A 6.2 mg amount of **16** (0.0050 mmol) was dissolved in 15 mL CH_2Cl_2 in a 50 mL three-neck flask and hydrogen was purged for 1 h at room temperature. The solvent was removed *in vacuo* and the products were separated by TLC by using 5/1 hexane/methylene chloride solvent mixture to yield a 3.0 mg amount (48%) of **17**.

2.11. Conversion of **17** to **18**

A 6.5 mg amount of **17** (0.0053 mmol) was dissolved in 15 mL CH_2Cl_2 in a 50 mL three-neck flask. A 6.6 µL (0.027 mmol) amount of PBu$_3^t$ was added to the solution and the solution was stirred at room temperature for 1 h. The solvent was removed *in vacuo* and the products were isolated by TLC by using 6/1 hexane/methylene chloride solvent mixture to yield a 3.1 mg (41%) of **18**.

2.12. Crystallographic analysis

Dark single crystals of **10**, red single crystals of **14**, dark single crystals of **13**, and dark single crystals of **18** suitable for diffraction analysis were grown by slow evaporation of solvent from a benzene/octane solution at 8 °C. Thin green plates of **11** suitable for diffraction analysis were grown by evaporation of solvent from a methylene chloride/hexane solution at room temperature. Golden yellow single crystals of **12** suitable for diffraction analysis were grown by slow evaporation of solvent from an ether solution at -25 °C. Dark single crystals of **16** and **17** suitable for diffraction analysis were grown by evaporation of solvent from a methylene chloride/hexane solution at -25 °C. Each data crystal was glued onto the end of thin glass fiber. X-ray intensity data were measured using a Bruker SMART APEX CCD-based diffractometer using Mo Kα radiation ($\lambda = 0.71073$ Å). The raw data frames were integrated with the SAINT+ program by using a narrow-frame integration algorithm [14]. Corrections for Lorentz and polarization effects were also applied by SAINT. An empirical absorption correction based on the multiple measurement of equivalent reflections was applied by using the program SADABS. All structures were solved by a combination of direct methods and difference Fourier syntheses, and refined by full-matrix least-squares on F^2, by using the SHELXTL software package [15]. All non-hydrogen atoms were refined with anisotropic displacement parameters. Unless indicated otherwise, all hydrogen atoms were placed in geometrically idealized positions and included as standard riding atoms. Crystal data, data collection parameters, and results of the analyses for compounds are listed in Tables 1 and 2.

Compounds **10**, **14**, and **17** all crystallized in the orthorhombic crystal system. For **10** the systematic absences were consistent with either of the space group *Pnn2* or

Table 1
Crystallographic data for compounds 10–13

Compound	10	11	12	13
Empirical formula	$Pt_2Os_3P_2O_{10}C_{34}H_{54} \cdot C_6H_6$	$Pt_2Os_3P_2O_{10}C_{34}H_{56}$	$Pt_2Os_3P_2O_{10}C_{34}H_{58} \cdot 1/2$ $(CH_3CH_2)_2O$	$PtOs_3PO_{10}C_{22}H_{27} \cdot 1/2$ C_6H_6
Formula weight	1723.60	1647.51	1686.58	1287.15
Crystal system	Orthorhombic	Monoclinic	Monoclinic	Triclinic
Lattice parameters				
a (Å)	12.8093(4)	27.9635(10)	16.7485(8)	9.1174(15)
b (Å)	20.1356(6)	20.7892(7)	15.9787(8)	12.723(2)
c (Å)	9.2275(3)	15.4264(6)	18.2023(9)	15.303(3)
α (°)	90	90	90	70.253
β (°)	90	105.650(1)	103.787(1)	82.942
γ (°)	90	90	90	72.112
V (Å^3)	2379.98(13)	8635.5(5)	4730.9(4)	1589.6(5)
Space group	$Pnn2$ (#34)	$P2_1/n$ (#14)	$P2_1/c$ (#14)	$P\bar{1}$ (#2)
Z value	2	8	4	2
ρ_{calc} (g/cm^3)	2.405	2.534	2.368	2.689
μ (Mo Kα) (mm^{-1})	13.953	15.376	14.037	16.437
Temperature (K)	294(2)	100(2)	150(2)	294(2)
$2\Theta_{max}$ (°)	56.6	56.0	56.6	56.5
No. of observed ($I > 2\sigma(I)$)	5272	11839	11063	5884
No. of parameters	252	916	504	358
Goodness-of-fit[a]	1.033	1.015	1.118	1.007
Maximum shift in cycle	0.001	0.002	0.003	0.001
Residuals[a]: R_1; wR_2	0.0304; 0.0605	0.0394; 0.0854	0.0229; 0.0573	0.0489; 0.1066
Absorption correction, Maximum/minimum	1.000/0.560	1.000/0.509	1.000/0.532	1.000/0.264
Largest peak in final difference map (e$^-$/ Å^3)	1.486	2.807	2.600	2.860

[a] $R = \Sigma_{hkl}(||F_{obs}| - |F_{calc}||)/\Sigma_{hkl}|F_{obs}|$; $R_w = [\Sigma_{hkl}w(|F_{obs}| - |F_{calc}|)^2/\Sigma_{hkl}wF_{obs}^2]^{1/2}$, $w = 1/\sigma^2(F_{obs})$; GOF $= [\Sigma_{hkl}w(|F_{obs}| - |F_{calc}|)^2/(n_{data} - n_{vari})]^{1/2}$.

Table 2
Crystallographic data for compounds 14 and 16–18

Compound	14	16	17	18
Empirical formula	$Os_3P_2O_{10}C_{34}H_{54}$	$PtOs_3PO_{10}C_{22}H_{29}$	$PtOs_3PO_9C_{21}H_{31}$	$PtOs_3P_2O_8C_{32}H_{54} \cdot 1/2C_6H_6$
Formula weight	1255.31	1250.11	1224.12	1433.44
Crystal system	Orthorhombic	Triclinic	Orthorhombic	Monoclinic
Lattice parameters				
a (Å)	14.0665(4)	8.9873(3)	13.5462(6)	14.8675(6)
b (Å)	15.9725(5)	11.3267(4)	16.9660(7)	16.5165(7)
c (Å)	18.2569(6)	15.7682(6)	12.7251(6)	17.5830(7)
α (°)	90	109.806(1)	90	90
β (°)	90	90.016(1)	90	90.179(1)
γ (°)	90	96.146(1)	90	90
V (Å^3)	4101.9(2)	1500.37(9)	2924.5(2)	4317.6(3)
Space group	$P2_12_12_1$ (#19)	$P\bar{1}$ (#2)	$Pna2_1$ (#33)	$P2_1/n$ (#14)
Z value	4	2	4	4
ρ_{calc} (g/cm^3)	2.033	2.767	2.780	2.205
μ (Mo Kα) (mm^{-1})	9.398	17.410	17.858	12.147
Temperature (K)	294(2)	294(2)	100(2)	100(2)
$2\Theta_{max}$ (°)	52.0	56.6	56.6	56.68
No. of observed ($I > 2\sigma(I)$)	6981	6422	6832	9823
No. of parameters	458	351	341	485
Goodness of fit[a]	1.059	1.066	1.083	1.133
Maximum shift in cycle	0.003	0.001	0.008	0.014
Residuals[a]: R_1; wR_2	0.0410; 0.0936	0.0245; 0.0611	0.0225; 0.0562	0.0301; 0.0680
Absorption correction, Maximum/minimum	1.000/0.717	1.000/0.458	1.000/0.485	1.000/0.532
Largest peak in final difference map (e$^-$/ Å^3)	2.137	1.477	0.806	2.646

[a] $R = \Sigma_{hkl}(||F_{obs}| - |F_{calc}||)/\Sigma_{hkl}|F_{obs}|$; $R_w = [\Sigma_{hkl}w(|F_{obs}| - |F_{calc}|)^2/\Sigma_{hkl}wF_{obs}^2]^{1/2}$, $w = 1/\sigma^2(F_{obs})$; GOF $= [\Sigma_{hkl}w(|F_{obs}| - |F_{calc}|)^2/(n_{data} - n_{vari})]^{1/2}$.

Pnnm. The structure could only be solved in the former space group. With $Z = 2$, the molecule lies on a 2-fold rotation axis and only one-half of the molecule is present in the asymmetric unit. There is also half a molecule of benzene from the crystallization solvent that co-crystallized with the complex that also lies on a 2-fold rotational axis. The

solvent molecule was included in the analysis and satisfactorily refined with isotropic thermal parameters. For compound **14** the space group $P2_12_12_1$ was identified on the basis of the systematic absences in the intensity data. The carbon atom C42 on the *t*-butyl group on atom P(2) was slightly disordered and was refined with one geometric restraint. The Flack parameter for this analysis was 0.00. For compound **17** the systematic absences were consistent with either of the space group $Pna2_1$ or $Pnma$. The structure could only be solved satisfactorily in the former space group. The four hydrido ligands were located, however H1 and H4 were refined with a fixed isotropic thermal parameter, while H2 and H3 were refined successfully with isotropic thermal parameters.

Compounds **11**, **12** and **18** crystallized in the monoclinic crystal system. For compound **11** the systematic absences in the intensity data uniquely identified the space group $P2_1/n$. With $Z = 8$ there are two independent molecules in the asymmetric unit. Despite many attempts, the crystals of **11** were obtained only as very thin plates. Carbon atoms C(14), C(36) and C(83) were refined with isotropic thermal parameters. The hydrido ligands were located crystallographically but were refined by using geometric restraints. For compound **12** the systematic absences in the intensity data uniquely identified the space group as $P2_1/c$. The hydrido ligands were located and refined with isotropic thermal parameter. The molecule co-crystallized with half a molecule of diethyl ether from the crystallization solvent. The solvent molecule was refined using one geometric restraint with isotropic thermal parameters. For compound **18** the space group $P2_1/n$ was identified uniquely by the pattern of systematic absences in the data. The tetrahedral Os$_3$Pt core is disordered over two orientations which were refined in the ratio 85/15. The disorder components were located from the difference map. The hydrido ligands were not located and were ignored in this structural analysis. The complex co-crystallized with half a molecule of benzene from the crystallization solvent lying about a center of symmetry. The solvent molecule was included and refined with isotropic thermal parameters.

Compounds **13** and **16** both crystallized in the triclinic crystal system. The space group $P\bar{1}$ was assumed and confirmed by the successful solution and refinement of the structures in both cases. Compound **13** co-crystallized with half a molecule of benzene from the crystallization solvent in the asymmetric crystal unit. The solvent molecule was included in the analysis and satisfactorily refined with isotropic thermal parameters. The hydrido ligand was located and refined on its positional parameters with a fixed isotropic thermal parameter. For compound **16** the hydrido ligands were located and refined successfully with isotropic thermal parameters.

2.13. Molecular orbital calculations

Single point molecular orbital calculations on compounds **10** and **11** were performed on the molecular structure as derived from the single crystal X-ray diffraction analysis. PH$_3$ was used in place of PBu$_3^t$ in these calculations. All molecular orbital calculations reported herein were performed by using the Fenske–Hall method [16]. The calculations were performed utilizing a graphical user interface developed [17] to build inputs and view outputs from stand-alone Fenkse-Hall (version 5.2) and MOPLOT2 binary executables [18]. Contracted double-ζ basis sets were used for the Os 5d, Pt 5d, P 3p, C 2p, O 2p and H 1s atomic orbitals. The Fenske–Hall scheme is a nonempirical approximate method that is capable of calculating molecular orbitals for very large transition metal systems and has built-in fragment analysis routines that allow one to assemble transition metal cluster structures from the ligand-containing fragments.

3. Results and discussion

The pentanuclear complex Pt$_2$Os$_3$(CO)$_{10}$(PBu$_3^t$)$_2$ (**10**) was the principal product (20% yield) obtained from the reaction of Pt(PBu$_3^t$)$_2$ with Os$_3$(CO)$_{10}$(NCMe)$_2$ at 0 °C. Three other products: PtOs$_3$(CO)$_{10}$(PBu$_2^t$)CMe$_2$CH$_2$(μ-H) (**13**) and Os$_3$(CO)$_{10}$(PBu$_3^t$)$_2$ (**14**) and Pt$_2$Os$_3$(CO)$_{10}$(PBu$_3^t$)(PBu$_2^t$)CMe$_2$CH$_2$(μ-H) (**15**) were obtained in lower yields of 7%, 8%, and 14%, respectively. Compounds **10**, **13** and **14** are new and were characterized by a combination of IR, ^{1}H and ^{31}P NMR, and a single-crystal X-ray diffraction analyses. Compound **15** was obtained previously from the reaction of Os$_3$(CO)$_{12}$ with Pt(PBu$_3^t$)$_2$ [2].

An ORTEP diagram of the molecular structure of **10** is shown in Fig. 1. Compound **10** consists of a trigonal bipy-
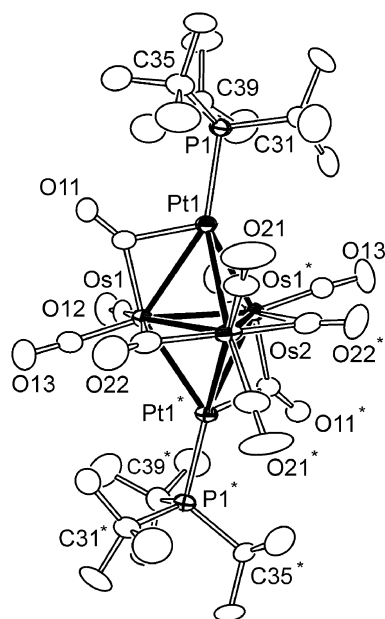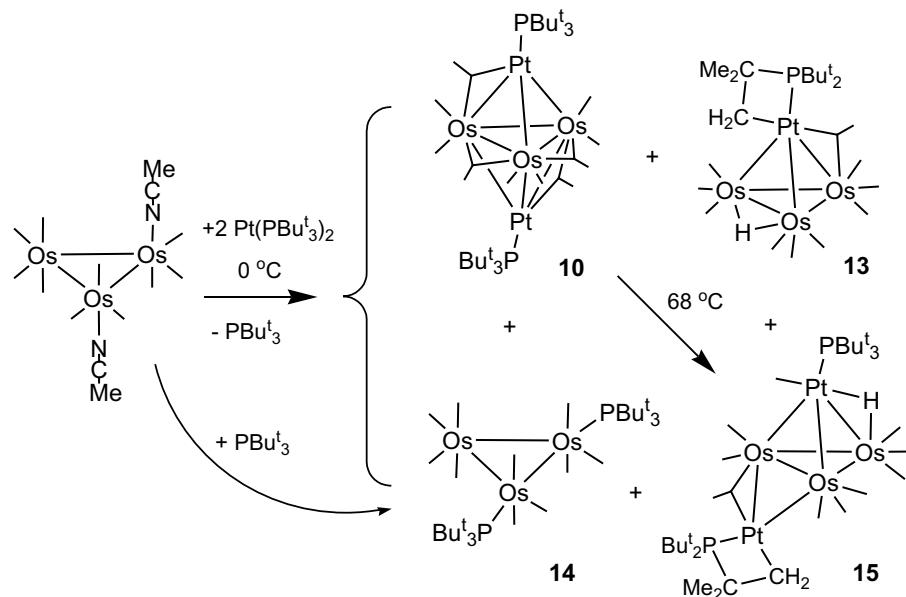

Fig. 1. ORTEP diagram of the molecular structure of Pt$_2$Os$_3$(CO)$_{10}$(PBu$_3^t$)$_2$ (**10**), showing 30% thermal probability thermal ellipsoids. Selected bond distances (in Å) are as follows: Pt(1)–P(1) = 2.3426(18), Pt(1)–Os(1) = 2.7923(3), Pt(1)–Os(1)* = 2.8104(4), Pt(1)–Os(2) = 2.8840(4), Os(1)–Os(2) = 2.8840(4), Os(1)–Pt(1)* = 2.8104(4), Os(1)–Os(1)* = 2.8590(6), Os(2)–Os(1)* = 2.7024(5), Os(1)–Pt(1)* = 2.8839(4).

Scheme 1.

ramidal cluster of five metal atoms. The three osmium atoms define the equatorial plane of the trigonal bipyramid. The platinum atoms occupy the apical positions. The molecule lies on a crystallographic twofold rotational axis that passes through the atom Os(2). Each platinum atom contains one PBu_3^t ligand. The complex has 10 CO ligands. Two are bridging ligands across Os–Os bonds. There is one bridging CO ligand to each platinum atom and the remainder are terminal ligands on the osmium atoms. The CO bridged Pt–Os bond distances, Pt(1)–Os(1) = 2.7923(3) Å, are significantly shorter than the unbridged ones, Pt(1)–Os(1)* = 2.8104(4) Å, Pt(1)–Os(2) = 2.8840(3) Å. The long length of the Pt(1)–Os(2) bond may be due to steric effects, as Os(2) is bonded to four CO ligands (including the bridging COs) and Os(1) has only three.

The total valence electron count for **10** is 68 electrons, which is 4 electrons less than the number expected for a trigonal bipyramidal cluster of five metal atoms according to the polyhedral skeletal electron pair theory [19]. This can be explained, however, if the two platinum atoms are assumed to have 16-electron configurations. Compound **10** can be converted to **15** in 50% yield simply by heating to 68 °C. Scheme 1 shows the products of this reaction and their relationships.

Compound **13** contains four metal atoms, one of platinum and three of osmium, arranged in a tetrahedral-type structure. An ORTEP diagram of the molecular structure of **13** is shown in Fig. 2. The PBu_3^t ligand is coordinated to the platinum atom and it is metallated on one of its methyl groups to form a four-membered ring with the platinum atom, Pt(1)–P(1)–C(49)–C(50), Pt(1)–C(50) = 2.085(10) Å. A similar metallated PBu_3^t is found in the five metal coproduct **15** [2]. Compound **13** contains one hydrido ligand, H(1), that was derived from the metallated

methyl group. The hydrido ligand was located and refined crystallographically, and it bridges the Os(2)–Os(3) bond, which is, as expected, longer than other Os–Os bonds: Os(2)–Os(3) = 2.7648(6) Å,   Os(1)–Os(2) = 2.7542(7) Å, Os(1)–Os(3) = 2.7546(6) Å [20]. Compound **8** contains a total of 58 cluster valence electrons which is two less than
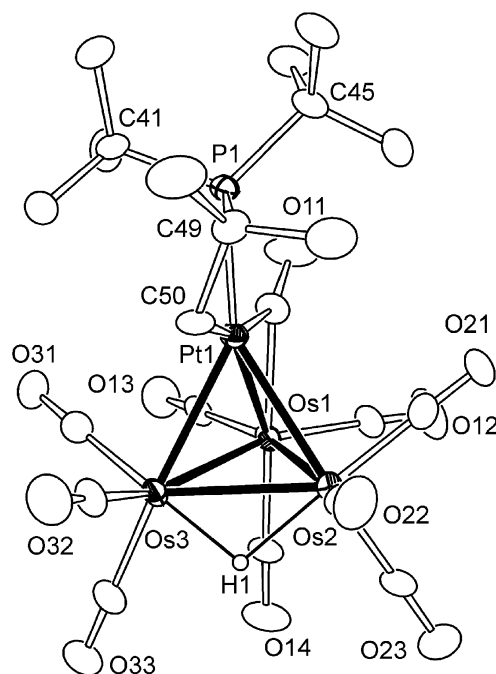

Fig. 2. An ORTEP diagram of the molecular structure of $PtOs_3(CO)_{10}(P-Bu_2^t)CMe_2CH_2(\mu-H)$ (**13**), showing 30% probability thermal ellipsoids. Selected bond distances (in Å) are as follows: Pt(1)–P(1) = 2.354(3), Pt(1)–C(50) = 2.085(10),   Pt(1)–Os(1) = 2.7723(6),   Pt(1)–Os(2) = 2.7763(6), Pt(1)–Os(3) = 2.7573(7), Os(1)–Os(2) = 2.7542(7), Os(1)–Os(3) = 2.7546(6), Os(2)–Os(3) = 2.7648(6).

the expected 60 electrons in which all metal atoms have 18 electron configurations. The 58-electron count can be explained by assuming that the platinum atom has a 16-electron configuration.

Compound **14** is a bis-PBu_3^t derivative of $Os_3(CO)_{12}$. It was characterized by IR, ^1H NMR and ^{31}P NMR spectroscopy, mass spectrum and by a single-crystal X-ray diffraction analysis. An ORTEP diagram of the molecular structure is shown in Fig. 3. The molecule contains two PBu_3^t ligands that lie in the plane of the Os_3 triangle. Both PBu_3^t ligands are positioned trans to the same metal–metal bond, Os(1)–Os(2), which is significantly longer than the other two Os–Os bonds, Os(1)–Os(2) = 2.9732(5) Å, Os(1)–Os(3) = 2.9361(6) Å, Os(2)–Os(3) = 2.9325(6) Å. The ^1H NMR spectrum of **14** exhibits a single very broad resonance at 1.55 ppm, $\Delta v_{1/2} = \sim 28$ Hz. The broadness of the ^1H resonance may be due to hindered rotations about the P–C bonds of the *t*-butyl phosphine ligands [21]. The $^{31}P\{^1H\}$ NMR spectrum shows a single sharp resonance at 76.7 ppm. Phosphine-substituted triosmium clusters have been fairly well studied [22]. Of the various possible isomers, in the structure of **14** and most other structurally characterized bis-phosphine derivatives of $Os_3(CO)_{12}$, the phosphine ligands tend to occupy equatorial sites trans to a metal–metal bond on adjacent metal atoms, structure **B** in Scheme 2 [22b].

In this reaction a PBu_3^t ligand is released by $Pt(PBu_3^t)_2$. It is possible that compound **14** was formed directly by the

reaction of $Os_3(CO)_{10}(NCMe)_2$ with PBu_3^t, and we have confirmed independently that compound **14** is obtained in good yield (75%) by this direct reaction. The reaction of $Os_3(CO)_{10}(NCMe)_2$ with $Pt(PBu_3^t)_2$ was performed at 0 °C in order to minimize the formation of **14**.

When solutions of **10** were exposed to hydrogen (1 atm) at 0 °C, two products were formed by the sequential addition of two equivalents of hydrogen to **10**. The first was a dihydrido complex $Pt_2Os_3(CO)_{10}(PBu_3^t)_2(\mu-H)_2$ (**11**), formed in 93% yield within 10 min. The molecular structure of **11** was established crystallographically. The crystal contains two complete formula equivalents of the molecule in the asymmetric unit. Both molecules are structurally similar. An ORTEP diagram of one of these (molecule 1) is shown in Fig. 4. The complex contains five metal atoms. One of the platinum atoms Pt(1) [Pt(4) in molecule 2] bridges an Os–Os edge of a tetrahedral $PtOs_3$ group of metal atoms. The cluster of **11** was formed by cleaving one of the Pt–Os bonds in the cluster of **10**. This Pt–Os distance was increased to over 4.00 Å, Os(1)$\cdots$Pt(1) = 4.057(1) Å [4.011(1) Å molecule 2]. Compound **11** contains two hydrido ligands. Both hydrido ligands were located structurally, but they were refined by using geometric restraints. One of these, H(1), bridges the Os–Os bond, Os(1)–Os(3). As expected, hydride-bridged bond is significantly longer, Os(1)–Os(3) = 2.9217(6) Å, than the other two Os–Os bonds, Os(1)–Os(2) = 2.7757(6) Å, Os(2)–Os(3) = 2.7104(6) Å [20]. The other hydride, H(2), bridges

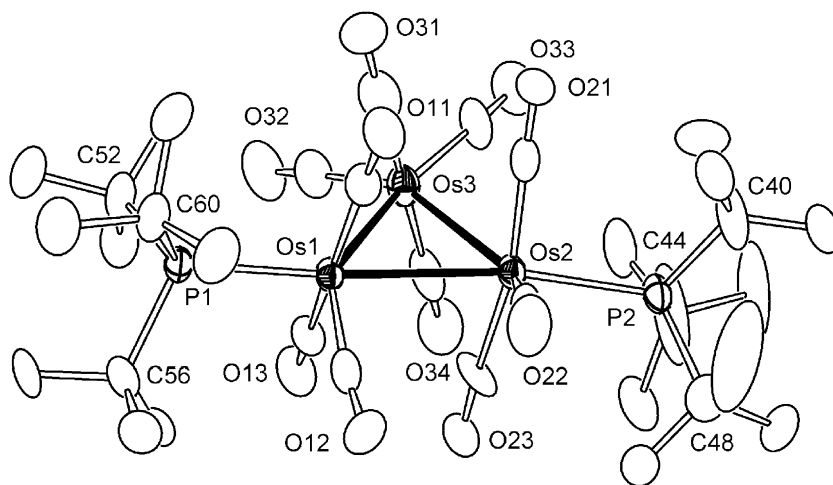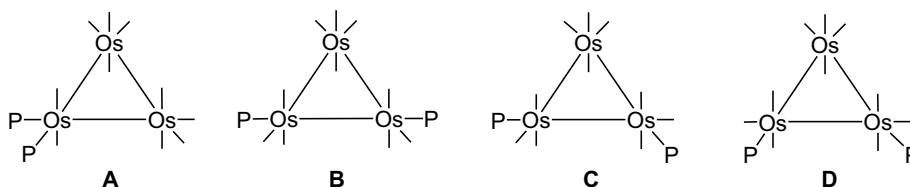Fig. 3. ORTEP diagram of the molecular structure of $Os_3(CO)_{10}(PBu_3^t)_2$ (**14**) showing 30% thermal probability thermal ellipsoids. Selected bond distances (in Å) are as follows: Os(1)–Os(2) = 2.9732(5), Os(1)–Os(3) = 2.9361(6), Os(2)–Os(3)= 2.9325(6), Os(1)–P(1) = 2.473(2), Os(2)–P(2) = 2.480(3).

Scheme 2.
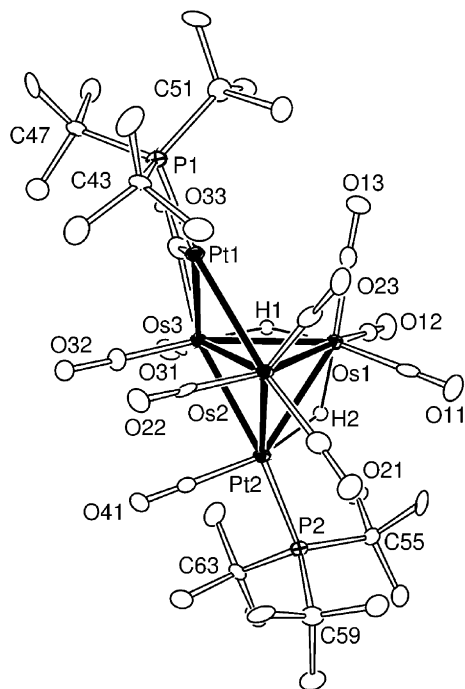
Fig. 4. ORTEP diagram of the molecular structure of $Pt_2Os_3(CO)_{10}$ $(PBu_3^t)_2(\mu\text{-H})_2$, **11** showing 70% thermal probability thermal ellipsoids. Selected bond distances (in Å) are as follows: (molecule 1) Os(1)$\cdots$Pt(1) = 4.057(1), Pt(1)–Os(2) = 2.8339(6), Pt(1)–Os(3) = 2.7353(6), Pt(1)–Os(2) = 2.8339(7), Pt(2)–Os(1) = 2.8821(6), Pt(2)–Os(2) = 2.8350(7), Pt(2)–Os(3) = 2.8093(6), Pt(2)–H(2) = 1.76(2), Os(1)–Os(2) = 2.7757(6), Os(1)–Os(3) = 2.9217(6), Os(1)–H(1) = 1.74(2), Os(1)–H(2) = 1.75(2), Os(2)–Os(3) = 2.7104(6), Os(3)–H(1) = 1.75(2), Pt(1)–P(1) = 2.298(3), Pt(2)–P(2) = 2.403(3); (molecule 2) Os(4)$\cdots$Pt(3) = 4.011(1), Pt(3)–Os(6) = 2.7521(6), Pt(3)–Os(5) = 2.8557(6), Pt(4)–Os(5) = 2.8242(6), Pt(1)–Os(6) = 2.8521(6), Pt(4)–Os(4) = 2.8642(6), Pt(4)–H(4) = 1.75(2), Os(4)–Os(5) = 2.7837(6), Os(4)–Os(6) = 2.9224(6), Os(4)–H(3) = 1.75(2), Os(4)–H(4) = 1.76(2), Os(5)–Os(6) = 2.7191(6), Os(6)–H(3) = 1.74(2), Pt(3)–P(3) = 2.304(3), Pt(4)–P(4) = 2.402(3).

the Pt–Os bond Pt(2)–Os(1), and this bond is also significantly longer, Pt(2)–Os(1) = 2.8821(6) Å, than the two unbridged Pt–Os bonds, Pt(2)–Os(2) = 2.8350(7) Å and Pt(2)–Os(3) = 2.8093(6) Å. The location of the hydrido ligands is further supported by the ^{1}H NMR spectrum which shows two highly-shielded resonances. The resonance at −10.49 ppm exhibits strong coupling to [195]Pt, $^1J_{Pt-H} = 559$ Hz, $^3J_{P-H} = 11$ Hz. This resonance is assigned to the bridging hydrido ligand on the Pt(2)–Os(1) bond. The resonance at −10.71 ppm exhibits small coupling to both platinum atoms, $^2J_{Pt-H} = 23$ Hz, $^2J_{Pt-H} = 25$ Hz, and is assigned to the bridging hydrido ligand on the Os(1)–Os(3) bond. The two hydrido ligands do not exhibit mutual coupling. The two PBu_3^t groups are chemically inequivalent in the solid state structure and the ^{1}H NMR shows two t-butyl resonances at $\delta = 1.34$ and 1.39. The ^{31}P NMR spectrum also shows two resonances at $\delta = 112.2$ and 117.6 with appropriate one bond coupling to [195]Pt, $^1J_{Pt-P} = 2787$ Hz, $^1J_{Pt-P} = 5579$ Hz, respectively. Compound **11** contains a total of 70 valance electrons. This is four electrons less than what would be expected for such a structure with all metal atoms having 18 electron config-

urations [19]. This deficiency can be explained by assuming that the two platinum atoms have 16-electron configurations.

The second hydrogen addition product, the tetrahydrido complex $Pt_2Os_3(CO)_{10}(PBu_3^t)_2(\mu\text{-H})_4$ (**12**), was obtained in 69% yield when hydrogen was purged through the solution of **11** for 80 min at 0 °C. Compound **12** was also obtained directly from **10** in 63% in one step under similar conditions. Compound **12** was characterized by IR, ^{1}H and ^{31}P NMR, and single-crystal X-ray diffraction analyses. An ORTEP diagram of the molecular structure of **12** is shown in Fig. 5. The structure of **12** contains a triangular Os_3 cluster with two $Pt(CO)(PBu_3^t)$ groups bridging adjacent edges of the triangle. Two Pt–Os bonds that were present in **10** were cleaved in the formation of **12**, Pt(2)$\cdots$Os(1) = 3.710(1) Å and Pt(1)$\cdots$Os(2) = 3.708(1) Å. Compound **12** contains four bridging hydrido ligands that were located and refined crystallographically. All four hydrido ligands bridge metal–metal bonds to atom Os(3). Due to the usual bond lengthening effect [20], the hydrogen-bridged Pt–Os bonds, Pt(1)–Os(3) = 2.8831(2) Å, Pt(2)–Os(3) = 2.8854(2) Å, are much longer than the Pt–Os bonds without bridging hydride ligands, Pt(1)–Os(3) = 2.7670(2) Å, Pt(2)–Os(3) = 2.7580(2) Å. Likewise, the hydride-bridged Os–Os bonds, Os(1)–Os(3) = 2.9349(2) Å and Os(2)–Os(3) = 2.9197(2) Å, are significantly longer than the unbridged bond Os(1)–Os(2) = 2.8590 Å. Due to second-order coupling,
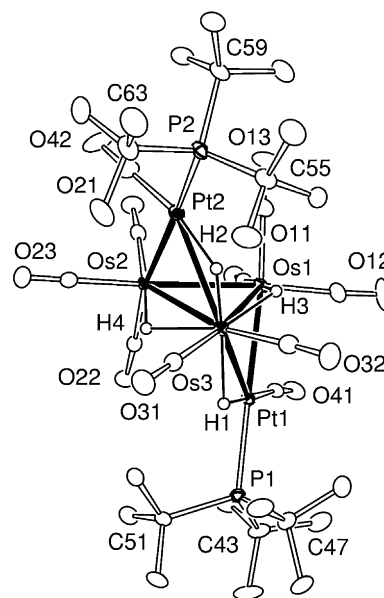
Fig. 5. ORTEP diagram of the molecular structure of $Pt_2Os_3(CO)_{10}(PBu_3^t)_2(\mu\text{-H})_4$, **12**, showing 30% thermal probability thermal ellipsoids. Selected interatomic distances (in Å) are as follows: Pt(2)$\cdots$Os(1) = 3.710(1) Å, Pt(1)$\cdots$Os(2) = 3.708(1) Å, Pt(1)–Os(1) = 2.7670(2), Pt(1)–Os(3) = 2.8831(2), Pt(1)–H(1) = 1.80(6), Pt(2)–P(2) = 2.3835(10), Pt(2)–Os(2) = 2.7580(2), Pt(2)–Os(3) = 2.8854(2), Pt(2)–H(2) = 1.78(6), Os(1)–Os(2) = 2.8590(2), Os(1)–Os(3) = 2.9349(2), Os(1)–H(1) = 1.67(5), Os(2)–Os(3) = 2.9197(2), Os(2)–H(4) = 1.55(5), Os(3)–H(1) = 1.85(6), Os(3)–H(2) = 1.61(6), Os(3)–H(3) = 1.82(5), Os(3)–H(4) = 1.98(5), Pt(1)–P(1) = 2.3746(10).

the ^1H NMR spectrum of **12** shows two complex multiplets in the hydride region. These were difficult to analyze due to multiple couplings. Note: although the two phosphines are symmetry equivalent they are magnetically nonequivalent. A ^{31}P decoupled ^1H NMR spectrum showed two hydride resonances at −9.01 ppm and −16.65 ppm. Each was a triplet, $^2J_{H-H} = 2.6$ Hz, due to H–H coupling. The resonance at −9.01 ppm was strongly coupled to platinum, $^1J_{Pt-H} = 421$ Hz. This is consistent with the structure found

in the solid state. The ^{31}P NMR spectrum shows a single peak at $\delta = 92.0$. Overall, this compound has a total of 72 valence electrons, which is four electrons less than expected according to the polyhedral skeletal electron pair theory for a triangle having two edge-bridging metal atoms [19].

Most interestingly, the addition of hydrogen to **10** is partially reversible. When solutions of **12** were purged with nitrogen for 10 h at 25 °C, compounds **10** and **11** were
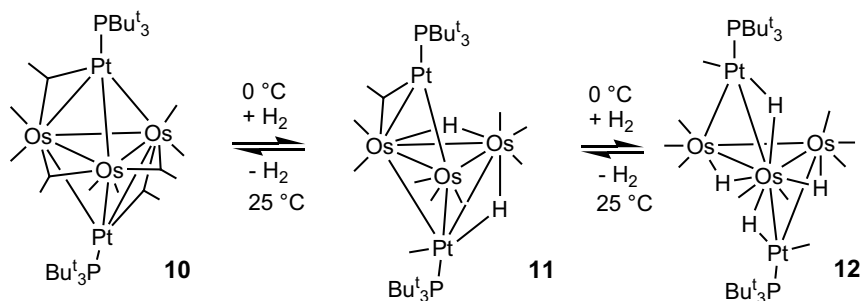
Scheme 3.
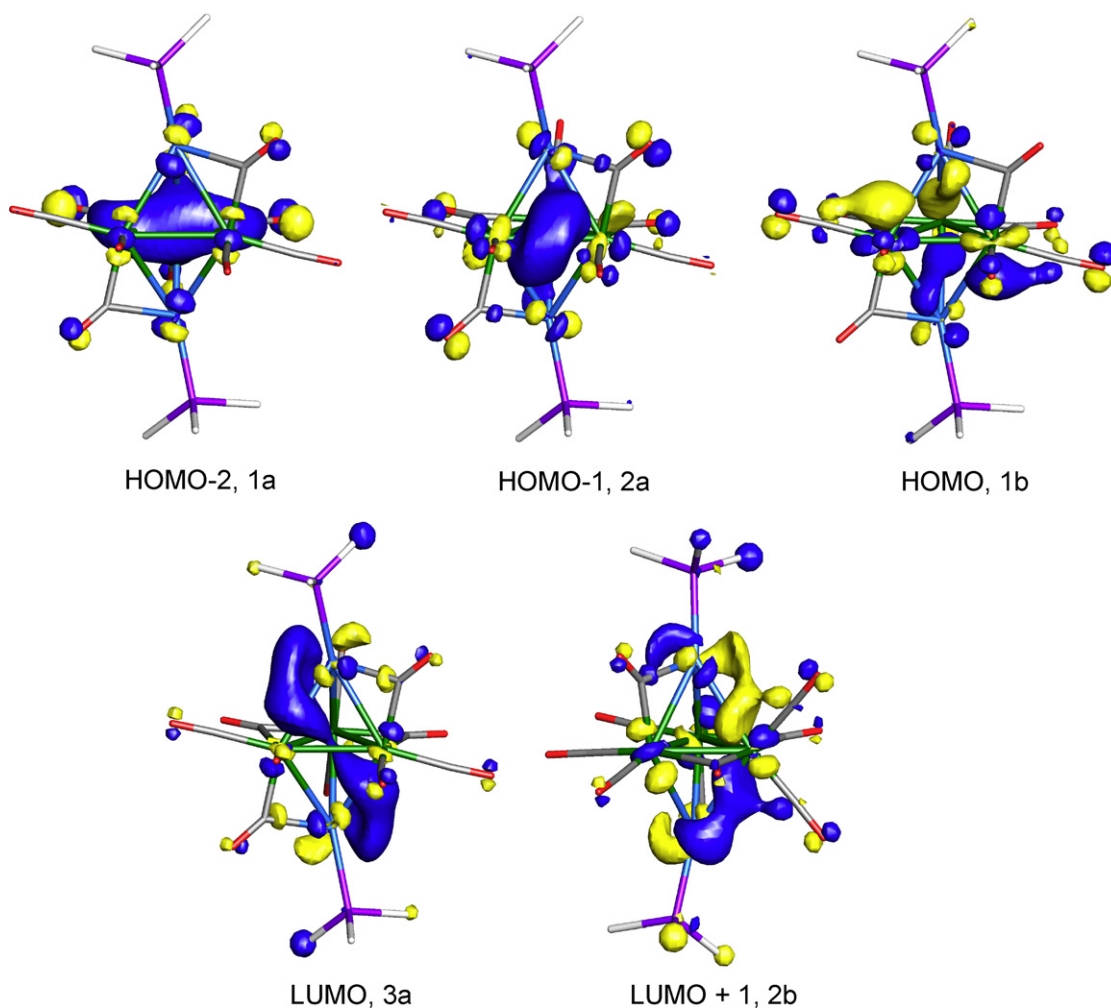
Fig. 6. Contour diagrams for some selected Fenske-Hall molecular orbitals for **10**.

formed and subsequently isolated in the yields 22% and 33%, respectively. 28% of the original amount of **12** was recovered in this experiment. When a solution of **12** was heated to 35 °C for 1 h in an NMR tube, compound **12** was converted back to **11** and **10** and molecular hydrogen was released and observed spectroscopically at 4.60 ppm. A schematic of the hydrogen addition/cluster transformation reactions reported here are shown in Scheme 3. With each addition of hydrogen, a Pt–Os bond to one of the Pt(PBu$_3^t$) groups is cleaved and the Pt(PBu$_3^t$) group is shifted to an edge of the cluster.

In order to gain a deeper understanding of the hydrogen addition process and the electronic structures of **10** and **11**, we have performed Fenske–Hall molecular orbital calculations on both compounds. Compound **10** possesses C_2 symmetry. Contour diagrams of the three highest occupied molecular orbitals HOMO 1b (−7.03 eV), HOMO−1 2a (−7.33 eV), HOMO−2 1a (−7.63 eV) and the two lowest unoccupied molecular orbitals LUMO 3a (−4.85 eV) and LUMO+1 2b (−4.24 eV) are shown in Fig. 6. The occupied molecular orbitals clearly are dominated by metal–metal bonding in the core of trigonal bipyramidal Os$_3$Pt$_2$ cluster.

The LUMO and LUMO+1, show that these orbitals are oriented predominantly along the Os–Pt bonds, see Fig. 6. It can be seen that a major component of the LUMO 3a is concentrated on the platinum atoms and the adjacent Pt–Os bond. Therefore, it seems most likely that the addition of hydrogen occurs at a platinum atom and may in turn induce cleavage of the proximate Pt–Os bond as electron density fills this virtual orbital and weakens the bond.

Compound **11** possesses only C_1 symmetry. Contour diagrams of the three highest occupied molecular orbitals HOMO 3a (−6.75 eV), HOMO−1 2a (−7.95 eV), HOMO−2 1a (−8.16 eV) and the lowest unoccupied molecular orbital LUMO 4a (−5.07 eV) are shown in Fig. 7. The HOMO 3a is dominated by metal–metal bonding interactions across the entire core of the Os$_3$Pt$_2$ cluster. The HOMO−1 2a and HOMO−2 1a also show significant metal–metal bonding interactions. The LUMO 4a is similar to the LUMO+1 2b in **10**. Furthermore, it can be seen that the major components of this orbital lie along three of the Os–Pt bonds, and it is one of these bonds, either Os(2)–Pt(2) or Os(3)–Pt(2) in **11**, see Fig. 4, that is cleaved to form
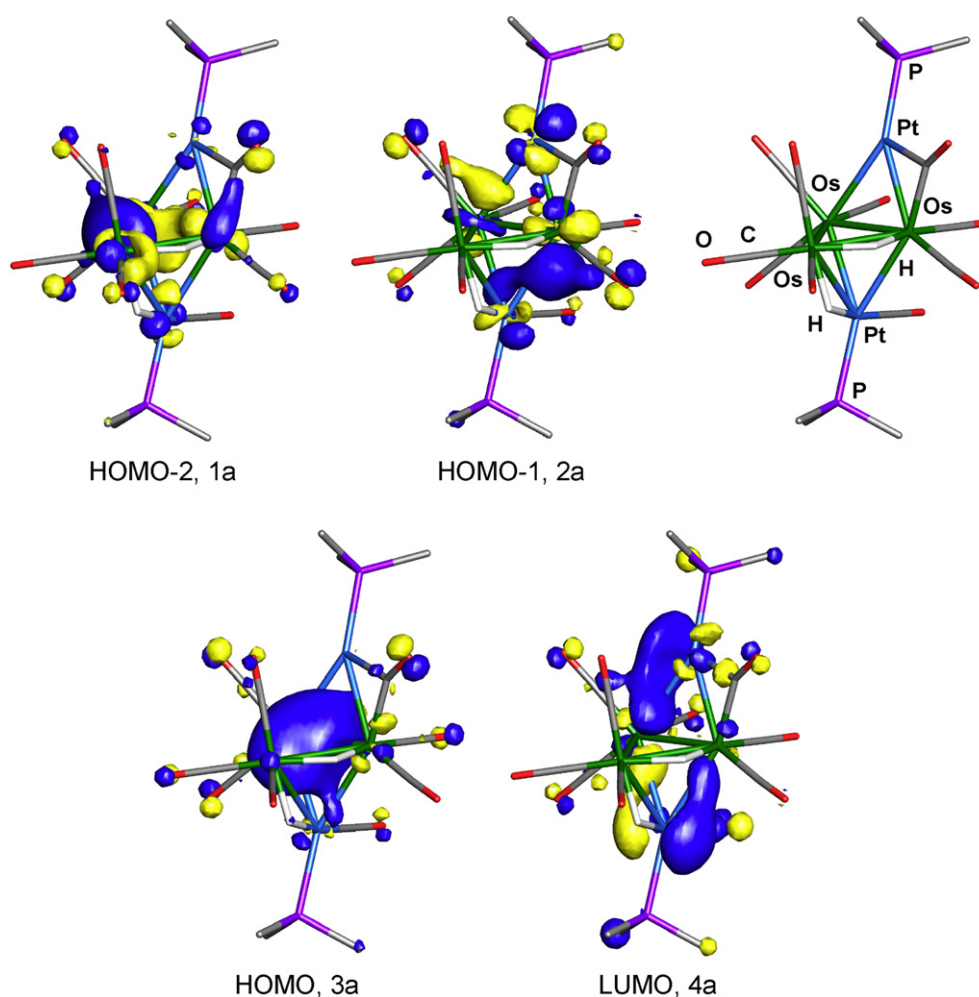

HOMO-2, 1a   HOMO-1, 2a

HOMO, 3a   LUMO, 4a

Fig. 7. Four contour diagrams for some selected Fenske-Hall molecular orbitals for **11**. Top right is a line structure showing the locations of the atoms in the diagrams.

the tetrahydrido cluster **12**. Thus, it seems most likely that hydrogen addition occurs at the platinum atom Pt(2).

Although **12** was still the major product (47% yield), three new tetranuclear metal compounds PtOs$_3$(CO)$_{10}$-(PBu$_3^t$)(μ-H)$_2$ (**16**), PtOs$_3$(CO)$_9$(PBu$_3^t$)(μ-H)$_4$ (**17**) and PtOs$_3$-(CO)$_8$(PBu$_3^t$)$_2$(μ-H)$_4$ (**18**), were obtained in low yields, 19%, 6% and 8%, respectively, when the reaction of **10** with hydrogen at 0 °C was performed over a period of 2.5 h. All three new compounds were characterized by a combination of IR, ^{1}H NMR and ^{31}P NMR, and single-crystal X-ray diffraction analyses.

Compound **16** consists of a tetrahedrally-shaped metal cluster containing one platinum and three osmium atoms. An ORTEP diagram of the molecular structure of **16** is shown in Fig. 8. The molecule contains two hydrido ligands, H(1) and H(2), that were located and refined crystallographically. Atom H(1) bridges the Pt(1)–Os(1) bond and atom H(2) bridges the Os(2)–Os(3) bond. As expected [20], both hydride-bridged metal–metal bonds, Pt(1)–Os(1) = 2.8613(3) Å and Os(2)–Os(3) = 2.7853(3) Å, are significantly longer than the unbridged metal–metal bonds, Pt(1)–Os(2) = 2.8133(3) Å, Pt(1)–Os(3) = 2.8189(3) Å, Os(1)–Os(3) = 2.7413(3) Å, and Pt(1)–Os(1) = 2.7472(3) Å. The ^{1}H NMR spectrum of **16** shows two highly-shielded resonances, $\delta = -7.24$ ppm and -8.14 ppm, that are attributed to the hydrido ligands. The resonance at -8.14 ppm exhibits strong coupling to ^{195}Pt ($^1J_{Pt-H} = 573$ Hz). Each osmium has three carbonyl ligands. The platinum atom
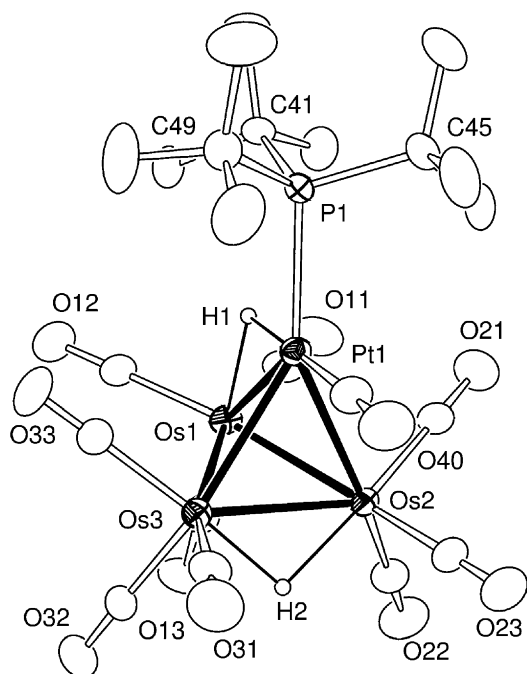
contains one terminal carbonyl ligand and the one PBu$_3^t$ ligand. This compound has a total of 58 valence electrons, which is two electrons less than the number expected for a tetrahedral structure of four metal atoms [19].

Compound **17** is structurally similar to that of **16**, except that it contains one less CO ligand and two more hydrido ligands than **16**. The presence of four hydrido ligands in **17** was confirmed by an electron impact mass spectrum which showed the parent ion at m/z 1224. Compound **17** was also obtained directly from **16** in 48% yield by reaction with hydrogen at 1 atm/25 °C for 1 h. Compound **17** was also characterized crystallographically and an ORTEP diagram of its molecular structure is shown in Fig. 9. The molecule contains a tetrahedrally-shaped PtOs$_3$ cluster with four hydrido ligands; all hydrido ligands were located but only H2 and H3 were refined crystallographically. In the solid state structure, two of the hydrido ligands bridge Os–Os bonds, one bridges one of the Pt–Os bonds, Pt(1)–Os(1), and one is terminally coordinated to the platinum atom Pt(1) and is positioned opposite to the Pt(1)–Os(1) bond. The hydride-bridged Pt(1)–Os(1) bond is much longer, 2.8766(4) Å, than the unbridged ones, Pt(1)–Os(2) = 2.7283(4) Å, Pt(1)–Os(3) = 2.7490(3) Å. The hydride-bridged Os–Os bond, Os(1)–Os(3) = 2.9302(4) Å, is also much longer than the other two Os–Os bonds, Os(1)–Os(2) = 2.8023(3) Å and Os(2)–Os(3) = 2.7898(4) Å. Curiously, however, one of latter two bonds, Os(2)–Os(3), also contains the bridging hydrido ligand H(4). There is no obvious explanation for the shortness of this bond [20].

Fig. 8. An ORTEP diagram of PtOs$_3$(CO)$_{10}$(PBu$_3^t$)(μ-H)$_2$ (**16**), showing 50% probability thermal ellipsoids. Selected bond distances (in Å) are as follows: Pt(1)–Os(1) = 2.8613(3), Pt(1)–Os(2) = 2.8133(3), Pt(1)–Os(3) = 2.8189(3), Os(1)–Os(2) = 2.7472(3), Os(1)–Os(3) = 2.7413(3), Os(2)–Os(3) = 2.7853(3), Pt(1)–H(1) = 1.72(6), Os(1)–H(1) = 2.06(6), Os(2)–H(2) = 1.87(6), Os(3)–H(2) = 1.81(6), Pt(1)–P(1) = 2.4282(13).
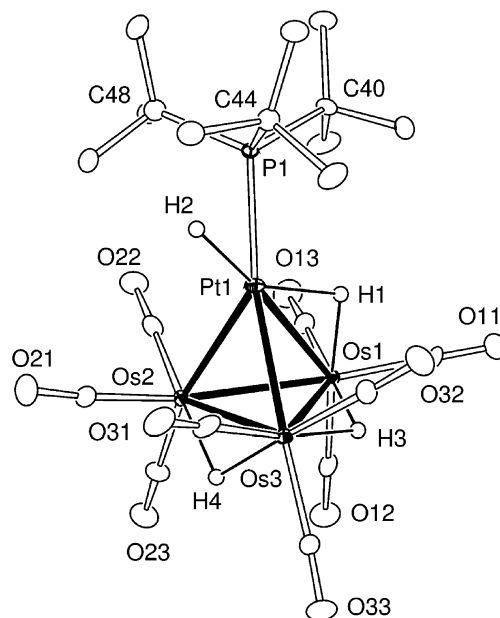
Fig. 9. An ORTEP diagram of PtOs$_3$(CO)$_9$(PBu$_3^t$)(μ-H)$_4$ (**17**), showing 50% probability thermal ellipsoids. Selected bond distances (in Å) are as follows: Pt(1)–P(1) = 2.3500(13), Pt(1)–H(1) = 1.92(8), Pt(1)–H(2) = 1.79(12), Pt(1) – Os(1) = 2.8766(4), Pt(1)–Os(2) = 2.7283(4), Pt(1)–Os(3) = 2.7490(3), Os(1)–H(1) =1.70(7), Os(1)–H(3) = 1.70(11), Os(1)–Os(2) = 2.8023(3), Os(1)–Os(3) = 2.9302(4), Os(2)–Os(3) = 2.7898(4), Os(2)–H(4) = 1.86(7), Os(3)–H(3) = 1.81(11), Os(3)–H(4) = 1.67(8).

In the solid state, the four hydrido ligands in **17** are inequivalent. Therefore, one would expect to see four separate hydride resonances in the ^{1}H NMR spectrum. However, only two resonances of equal intensity were observed in the hydride region of the spectrum, −10.72 ppm (d, 2 H, hydride, $^1J_{Pt-H} = 759$ Hz) and −16.62 ppm (d, 2H, hydride, $^2J_{Pt-H} = 14$ Hz, $^3J_{P-H} = 1.5$ Hz). Assuming the possibility of a dynamical averaging process, a ^{1}H NMR spectrum of **17** was recorded at −90 °C, the lowest temperature that we could obtain, to try to obtain evidence for this. At −90 °C, the hydride resonances were very broad. This is consistent with a very rapid dynamical averaging process; however, activation parameters can not be calculated in the absence of a rate-limiting low temperature spectrum.

A very simple exchange mechanism is proposed that allows for the interchange of the two platinum-coordinated hydrido ligands, see Scheme 4. The terminal ligand H(2) on Pt is shifted to an edge-bridging position across the Pt(1)–Os(2) bond and simultaneously the bridging ligand H(1) is shifted to a terminal position on Pt(1) by breaking the Os(1)–H(1) bond to form **17b**. This exchange process also leads to an exchange of the environments of the hydrido ligands H(3) and H(4) that are coordinated to the two osmium atoms. Compound **17** has a total of 58 valence electrons, which is two electrons less than the number expected for a tetrahedron of four metal atoms.

Compound **18** is a PBu$_3^t$ derivative of **17**, and it was also obtained in 41% yield directly from **17** by reaction with PBu$_3^t$ at room temperature. An ORTEP diagram of the molecular structure of **18** is shown in Fig. 10. The molecular structure of **18** consists of a tetrahedral PtOs$_3$ cluster with two PBu$_3^t$ ligands. As in **17**, one of the PBu$_3^t$ ligands is coordinated to the platinum atom. The other one is coordinated to an osmium atom, Os(3). Compound **18** contains a minor component of disorder (15%) in the solid state. Only the metal atoms of the disordered component were located and refined. As a result, the hydrido ligands of the major component were not observed in the analysis. However, on the basis of a comparison of the structures of **17** and **18**, it is believed that the hydrido ligands occupy positions in **18** that are similar to those in **17**, that is, there is a terminal hydrido ligand on Pt(1), trans to the Pt(1)–
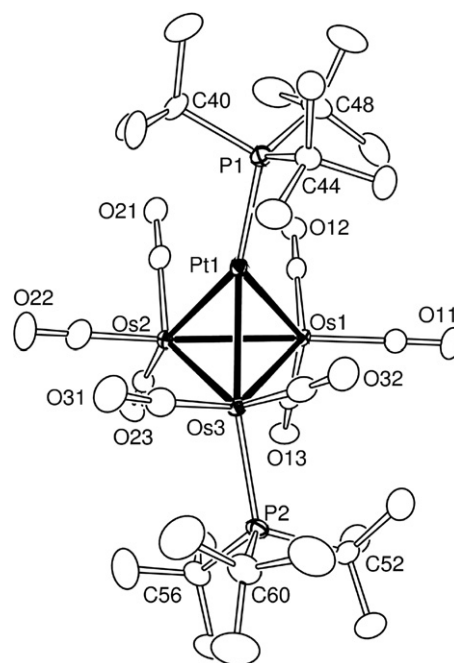

Fig. 10. An ORTEP diagram of PtOs$_3$(CO)$_8$(PBu$_3^t$)$_2$(µ-H)$_4$ (**18**), showing 50% probability thermal ellipsoids. Selected bond distances (in Å) are: Pt(1)–Os(1) = 2.8775(13), Pt(1)–Os(2) = 2.7496(12), Pt(1)–Os(3) = 2.7697(9), Os(1)–Os(2) = 2.8181(11), Os(1)–Os(3) = 2.9712(10), Os(2)–Os(3) = 2.7672(8), Pt(1)–P(1) = 2.3260(16), Os(3)–P(2) = 2.4390(13).

Os(1) bond and also a bridging hydrido ligand across the Pt(1)–Os(1) bond. As in **17**, the Pt(1)–Os(1) bond in **18**, 2.8775(13) Å, is significantly longer than the other two Pt–Os bonds, Pt(1) - Os(2) = 2.7496(12) Å, Pt(1)–Os(3) = 2.7697(9) Å. It is believed that the two remaining hydrido ligands bridge the Os(1)–Os(3) and Os(2)–Os(3) bonds as in **17**. This is supported by the very long length of the Os(1)–Os(3) bond, 2.9712(10) Å. As in **17**, the Os(2)–Os(3) bond is inexplicably short, 2.7672(8) Å. As in **17**, only two resonances of equal intensity were observed for the hydrido ligands in the ^{1}H NMR spectrum of **18**, −10.18 ppm ($^2J_{P-H} = 9.7$ Hz, $^3J_{P-H} = 1.5$ Hz, $^1J_{Pt-H} = 755$ Hz) and −13.96 ppm ($^2J_{P-H} = 6.4$ Hz, $^2J_{Pt-H} = 13$ Hz), one exhibits large coupling to ^{195}Pt and the other does not. The ^{31}P NMR spectrum shows two doublets, one at 81.5 ppm and another at 124.2 ppm which are mutually coupled, $^3J_{P-P} = 30$ Hz. The resonance at 124.2 ppm also exhibits strong coupling to ^{195}Pt, $^1J_{Pt-P} = 3370$ Hz, and is assigned to the phosphorus atom bonded directly to the platinum atom, P(1) in Fig. 10. In the ^{1}H coupled ^{31}P NMR spectrum, each phosphorus resonance was observed as a doublet of triplets due to coupling from hydride ligands, indicating there are two sets of two equivalent hydrido ligands in this cluster. Compound **18** has a total of 58 valence electrons, two electrons less than the number expected for a tetrahedral cluster of four metal atoms [19].

Scheme 5 shows the tetranuclear products **16–18** and their relationships. Compound **16** appears to be the first one from by degradation of the pentanuclear clusters in

17a   **17b**
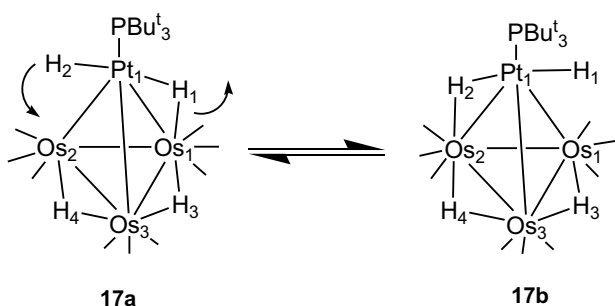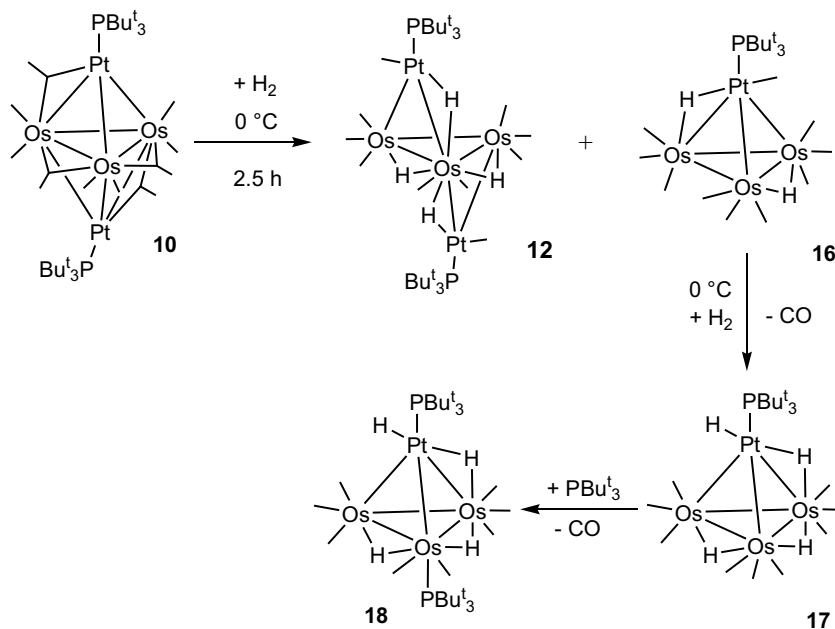
Scheme 4.

Scheme 5.

the course of their reactions with hydrogen. This is consistent with the observation of Pt–Os bond cleavage processes that occur in the formation of **11** and **12** when hydrogen is added to **10**.

4. Summary

We have shown that the unsaturated bimetallic cluster complex **10** is formed by the reaction of $Os_3(CO)_{10}$-$(NCMe)_2$ with $Pt(PBu_3^t)_2$. Compound **10** contains two triply bridging $Pt(PBu_3^t)$ groups giving an overall trigonal bipyramidal shape to the cluster of five metal atoms. Compound **10** adds hydrogen under mild conditions, e.g., 0 °C, by a series of Pt–Os bond cleavage processes to yield the di- and tetrahydrido compounds **11** and **12**. These additions are partially reversible. On longer exposure to hydrogen, the clusters begin to degrade by loss of a platinum phosphine group. The activation of hydrogen is an important first step in most catalytic hydrogenation reactions. Bi- and multimetallic cluster complexes have been shown to be precursors for the efficient preparation of bi- and multimetallic nanoparticles for use in catalytic hydrogenation reactions [23].

Acknowledgements

Appendix A. Supplementary data

The crystallographic data has been deposited as follows: CCDC 641569 for **12**, CCDC 641570 for **14**, CCDC 641571 for **10**, CCDC 641572 for **11**, CCDC 655100 for **13**, CCDC 655101 for **16**, CCDC 655102 for **17**, CCDC 655108 for **18**. These data can be obtained free of charge via http://www.ccdc.cam.ac.uk/conts/retrieving.html, or from the Cambridge Crystallographic Data Centre, 12 Union Road, Cambridge CB2 1EZ, UK; fax: (+44) 1223-336-033; or e-mail: deposit@ccdc.cam.ac.uk. Supplementary data associated with this article can be found, in the online version, at doi:10.1016/j.jorganchem.2007.08.006.

References

[1] (a) R.D. Adams, B. Captain, W. Fu, M.B. Hall, J. Manson, M.D. Smith, C.E. Webster, J. Am. Chem. Soc. 126 (2004) 5253–5267;
    (b) R.D. Adams, B. Captain, W. Fu, M.D. Smith, J. Am. Chem. Soc. 124 (2002) 5628–5629.
[2] R.D. Adams, B. Captain, W. Fu, M.D. Smith, L. Zhu, Inorg. Chem. 45 (2006) 430–436.
[3] (a) R.D. Adams, B. Captain, P.J. Pellechia, J.L. Smith Jr., Inorg. Chem. 43 (2004) 2695–2702;
    (b) R.D. Adams, B. Captain, M.B. Hall, J.L. Smith Jr., C.E. Webster, J. Am. Chem. Soc. 127 (2005) 1007–1014;
    (c) R.D. Adams, B. Captain, L. Zhu, J. Cluster Sci. 17 (2006) 87–95.
[4] R.D. Adams, B. Captain, Mark D. Smith, C. Beddie, M.B. Hall, J. Am. Chem. Soc. 129 (2007) 5981–5991.
[5] (a) R.D. Adams, B. Captain, C. Beddie, M.B. Hall, J. Am. Chem. Soc. 129 (2007) 986–1000;
    (b) R.D. Adams, B. Captain, Angew. Chem., Int. Ed. 44 (2005) 2531–2533.
[6] (a) G.W. Crabtree, M.S. Dresselhaus, M.V. Buchanan, Phys. Today (2004) 39–44;

(b) J.M. Ogden, Phys. Today 55 (2002) 69–75;
(c) P.P. Edwards, V.L. Kuznetsov, W.I.F. David, Phil Trans. R. Soc. A 365 (2007) 1043–1056.

[7] (a) L. Schlapbach, A. Züttel, Nature 414 (2001) 353;
(b) N.L. Rosi, J. Eckert, M. Eddaoudi, D.T. Vodak, M. O'Keerre, O.M. Yaghi, Science 300 (2003) 1127;
(c) X. Zhao, B. Xiao, A.J. Fletcher, K.M. Thomas, D. Bradshaw, M.J. Rosseinsky, Science 306 (2004) 1012.

[8] (a) J.N. Armor, Catal. Lett. 101 (2005) 131–135;
(b) J.M. Thomas, R. Raja, B.F.G. Johnson, S. Hermans, M.D. Jones, T. Khimyak, Ind. Eng. Chem. Res. 42 (2003) 1563–1570.

[9] (a) G.J. Kubas, Metal Dihydrogen and σ-Bond Complexes, Kluwer Academic/Plenum Publishers, New York, 2001;
(b) D.M. Heinekey, A. Lledos, J.M. Lluch, Chem. Soc. Rev. 33 (2004) 175–182.

[10] (a) P.J. Dyson, S.J. McIndoe, Angew. Chem., Int. Ed. 44 (2005) 5772–5774;
(b) S.K. Brayshaw, M.J. Ingleson, J.C. Green, J.S. McIndoe, P.R. Raithby, G. Kociok-Köhn, A.S. Weller, J. Am. Chem. Soc. 128 (2006) 6247–6263;
(c) R.D. Adams, B. Captain, M.D. Hall, C. Beddie, M.B. Hall, J. Am. Chem. Soc. 129 (2007) 5981–5991.

[11] R.D. Adams, B. Captain, L. Zhu, J. Am. Chem. Soc. 129 (2007) 2454–2455.

[12] P.A. Dawson, B.F.G. Johnson, J. Lewis, J. Puga, P. Raithby, M.J. Rosales, J. Chem. Soc., Dalton Trans. (1982) 233.

[13] R.D. Adams, B. Captain, W. Fu, M.D. Smith, L. Zhu, Inorg. Chem. 45 (2006) 430.

[14] SAINT+ Version 6.2a. Bruker Analytical X-ray System, Inc., Madison, WI, USA, 2001.

[15] G.M. Sheldrick, SHELXTL Version 6.1, Bruker Analytical X-ray Systems, Inc., Madison, WI, USA, 1997.

[16] M.B. Hall, R.F. Fenske, Inorg. Chem. 11 (1972) 768.

[17] J. Manson, C.E. Webster, M.B. Hall, JIMP, development version 0.1.v117 (built for Windows PC and Redhat Linux); Department of Chemistry, Texas A& M University: College Station, TX; <http://www.chem.tamu.edu/jimp/> (accessed July 2004).

[18] MOPLOT2 for orbital and density plots from linear combinations of Slater or Gaussian type orbitals, version 2.0; D.L. Lichtenberger, Department of Chemistry, University of Arizona: Tucson, AZ, 1993.

[19] D.M.P. Mingos, Accts. Chem. Res. 17 (1984) 311.

[20] (a) R. Bau, M.H. Drabnis, Inorg. Chim. Acta 259 (1997) 27–50;
(b) R.G. Teller, R. Bau, Struct. Bond. 41 (1981) 1.

[21] (a) C.D. Rithner, C.H. Bushweller, J. Am. Chem. Soc. 107 (1985) 7823;
(b) C.H. Bushweller, J.A. Brunelle, J. Am. Chem. Soc. 95 (1973) 5949.

[22] (a) M.I. Bruce, M.J. Liddell, C.A. Hughes, J.M. Patrick, B.W. Skelton, A.H. White, J. Organomet. Chem. 347 (1988) 181;
(b) W.K. Leong, Y. Liu, J. Organomet. Chem. 584 (1999) 174;
(c) A.J. Deeming, in: E.W. Abel, F.G.A. Stone, G. Wilkinson (Eds.), Comprehensive Organometallic Chemistry II, vol. 7, Elsevier, Oxford, 1995 (Chapter 12).

[23] (a) J.M. Thomas, B.F.G. Johnson, R. Raja, G. Sankar, P.A. Midgley, Accts. Chem. Res. 36 (2003) 20–30;
(b) A.B. Hungria, R. Raja, R.D. Adams, B. Captain, J.M. Thomas, P.A. Midgley, V. Golvenko, B.F.G. Johnson, Angew. Chem., Int. Ed. 45 (2006) 4782–4785;
(c) O. Alexeev, B.C. Gates, Ind. Eng. Chem. Res. 42 (2003) 1571–1587.